Appl. Phys. A (2017) 123:106
DOI 10.1007/s00339-016-0671-x

Applied Physics A
Materials Science & Processing

Effect of external applied steady magnetic field on the morphology of laser welding joint of 4-mm 2024 aluminum alloy

Xiaohong Zhan[1,2] · Junjie Zhou[1] · Weihua Sun[2] · Jicheng Chen[1] · Yanhong Wei[1]

Received: 8 November 2016 / Accepted: 8 December 2016 / Published online: 2 January 2017

Abstract Additional external steady magnetic fields were applied to investigate the influence of a steady magnetic field aligned perpendicular to the welding direction during laser beam welding of 2024 aluminum alloy. The flow pattern in the molten pool and the weld seam geometry were significantly changed by the induced Lorentz force distribution in the liquid metal. It revealed that the application of a steady magnetic field to laser beam welding was helpful to the suppression of the characteristic wineglass-shape and the depth-to-width ratio because of the Marangoni convection. The microstructures and component distributions at various laser power and magnetic field intensity were analyzed too. It was indicated that the suppression of the Marangoni convection by Lorentz force was beneficial to accumulation of component and grain coarsening near the fusion line.

1 Introduction

In the past years, current trends in modern lightweight designs show an increasing application of high-strength but thin sheeted aluminum. Thin sheeted AA2024 has been generally considered as a valuable structural material with extensive application in aerospace, navigation and automobile industry due to its high strength and fatigue strength [1, 2]. As a typical kind of the Al–Cu–Mg series alloy, the performance of AA2024 relies heavily on 3.8–4.9% cuprum and 1.2–1.8% magnesium (wt%), resulting in good mechanical properties, formability and weldability [3].

Arc welding had been commonly employed for AA2024 joining in the industries. However, the application of AA2024 is confined by the significant deformation and metallurgical reaction (resulting in crack, porosity, grain coarsening, for example) due to high heat input and low welding speed [4, 5]. The problems in the arc welding can be solved effectively by using laser beam welding (LBW). The weld formation, process parameters, properties, microstructure and numerical simulation on laser beam welding of aluminum alloy have been discussed by considerable studies [6–11]. Nevertheless, the typical wineglass-shape of the weld cross sections, as a common problem on high-penetration-depth laser welding of aluminum alloy, occurred inevitably [12]. A residual stress is left after cooling due to the wineglass-shape [13].

Extensive studies on laser welding under the influence of magnetic field [14–23] have been reported where mechanism, weld formation and numerical simulation were discussed, but few of them were related to constant magnetic field and thin sheeted aluminum alloy. A Schneider [24] studied the laser beam welding of 6-mm $AlMg_3$ under the influence of AC magnet where the effect of magnetic field on the weld pores and weld surface roughness was analyzed. Bachmann et al. [17] and Avilov et al. [18] focused on the interaction between the AC magnetic field and convection. In [19], a numerical simulation of flow field in the molten pool was studied to find out the optimal magnetic flux density to inhibit the convection. In addition, reliable experiments of laser beam welding of thick aluminum were analyzed to prove its opinions.

✉ Xiaohong Zhan
xiaohongzhan_nuaa@126.com

[1] College of Material Science and Technology, Nanjing University of Aeronautics and Astronautics, Nanjing 211106, China

[2] Department of Materials Science and Engineering, The Ohio State University, Columbus, OH 43210, USA

To obtain an in-depth understanding of LBM under the influence of steady magnetic field for thin sheeted AA2024, more profound efforts on the weld formation and mechanisms of action are supposed to be made. From these points, the morphology of cross section, microstructure and the distribution of alloying component in the welds are important because of their tight correlations with molten convection during welding process. Partly related investigations have been performed in previous studies on melt pool convections during the laser beam welding process [25–29].

In this paper, 4-mm AA2024 plates were laser-beam-welded under the influence of steady magnetic field. Welding parameters are optimized for desired welding stability. In addition, the magnetic field intensity is projected for obvious improvement. The microstructure of critical regions including heat-affected zone (HAZ) and fusion zone (FZ) and the width-to-depth ratio of weld seam were explored. Besides, the component distribution was qualitatively analyzed.

2 Experiment design

In this paper, the transverse magnetic field is formed by two identical independent square magnets; thereafter, a spindle shaped magnetic field is generated between the two poles. The 2024 aluminum alloy plate is arranged between the two magnetic poles as shown in Fig. 1.

It is well known that a significant effect on the dynamics of the flow behavior appeared after the application of magnetic fields in the presence of electrically conducting liquids. This paper focuses on the interaction between Marangoni convection and the magnetic field as shown in Fig. 2a. In the weld molten pool, due to the non-uniform gravity field, thermal field, surface tension and other factors, welding pool flows become very complex. There are mainly two forms of convection: Marangoni and natural convection, and are shown in Fig. 2b.

The Marangoni effect which occurs near the surface region becomes dominant. It leads to comparatively large weld bead and the typical wineglass-shape of the weld cross sections, which is common for the laser beam welding of aluminum alloy. Additionally, natural convection in the melt due to the thermal expansion of the material when exposed to high temperature differences also plays an important role, especially in deep regions of the weld pool. Both together lead to an unstable behavior of the weld pool surface.

The movement of Marangoni convection perpendicular to a magnetic field induces an electric current density

$$\vec{J} = \sigma\left(\vec{E} + \vec{v} \times \vec{B}\right) \tag{1}$$

The electric current interacts with the externally applied magnetic field, and a Lorentz force distribution arises

$$\vec{F} = \vec{J} \times \vec{B} \tag{2}$$

where σ is conductivity, v is melt flow velocity, and B is magnetic field intensity. The direction of induced Lorentz force is opposite to the direction of Marangoni convection that is directed against the fluid flow. Hence, a dissipating effect appears.

A welding platform is designed by non-magnetic material to prevent the interference of magnetic field. The welding equipment is shown in Fig. 3. The welding parameters are decided by the previous research work. X. H. Zhan et al. studied the influence of laser welding parameters on the performance of thin sheeted aluminum

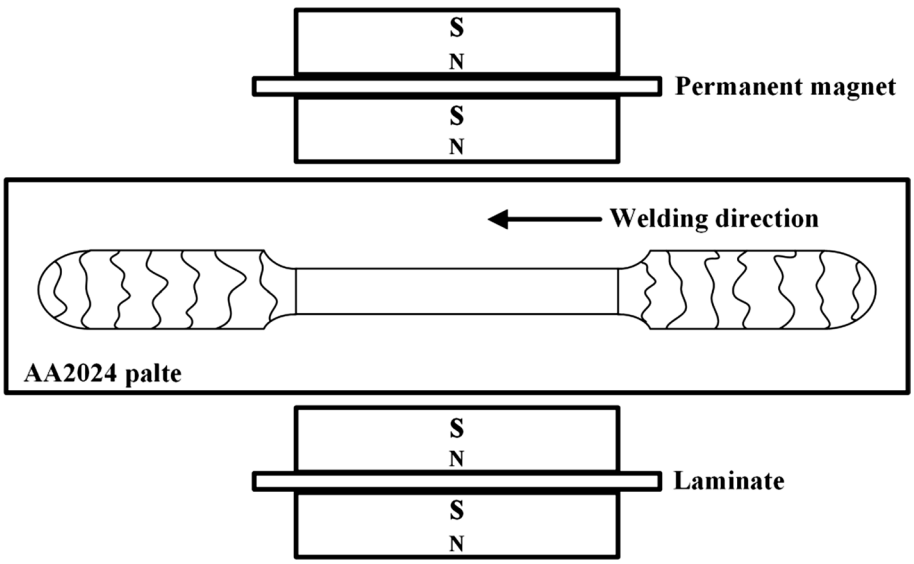

Fig. 1 Schematic diagram of laser welding under magnetic field

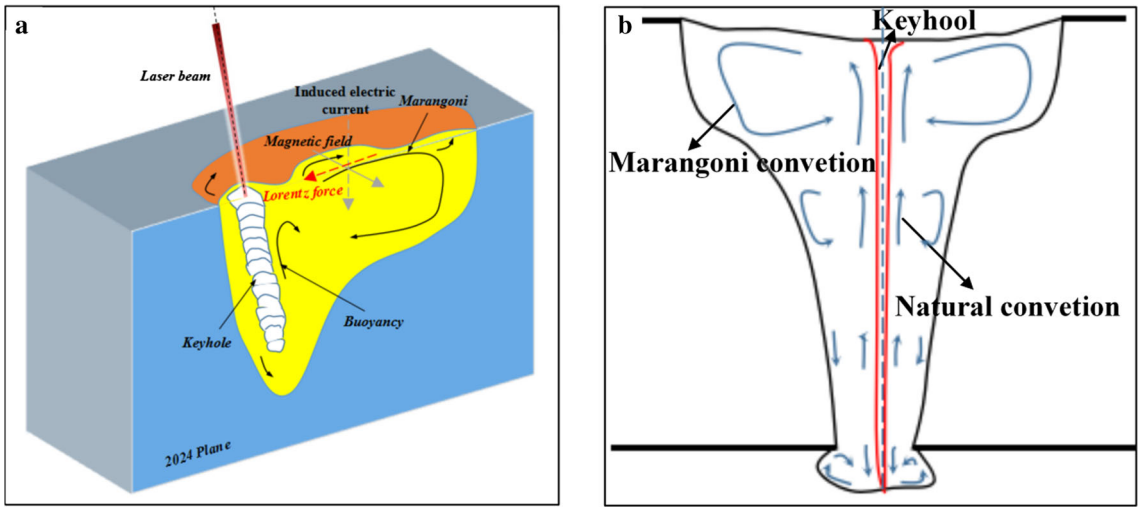

Fig. 2 Magnetic and flow field sketch: **a** interaction between magnetic and flow field; **b** convection in weld pool

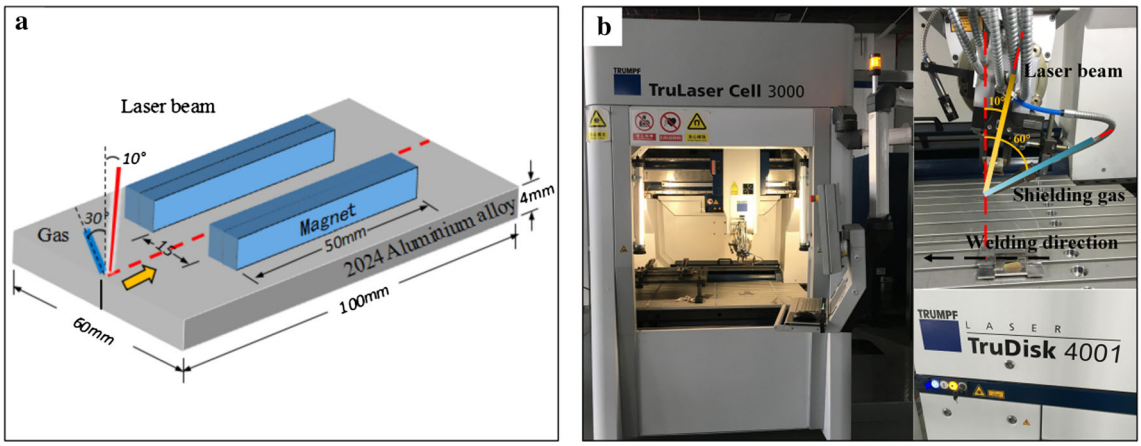

Fig. 3 Schematic diagram of experimental device

Table 1 Chemical composition of AA2024

Component	Cu	Mg	Mn	Zn	Cr	Al
wt%	3.81	1.72	0.44	0.25	0.10	Bal

alloy. It was found that a stable and effective welding process was taken when then laser power was around 2000 W. In this paper, the laser power was defined as 2200 and 2600 W.

Thin rolled sheets of 2024 aluminum alloy were used as parent material. 2024 aluminum alloy plates of dimensions 100 mm × 60 mm × 4 mm were welded by the laser beam welding. The chemical composition of AA2024 is shown in Table 1.

Based on the two key variables, that is laser power and magnetic field intensity, the experiments are divided into six groups as shown in Table 2. The average welding parameters are shown as follows.

Welding speed: 1.5 m/min, spot diameter: 480 μm, protection gas flow: 15 L/min (Ar), defocusing amount: −1 mm.

Surface cleanup treatment for the metal base prior to welding is indispensable for obtaining a high welding quality. The processes involve mechanically abrading, acid pickling and acetone cleaning. After welding, the macro-performance of the welds was captured by CCD camera.

3 Results

The welding parameters for six experimental cases gain access to a partial penetration and a full penetration of AA2024 welds with no crack.

As shown in Fig. 4a, b, the weld surface comes along with strong spattering and ejection shows the instability during laser beam welding of AA2024. For the laser welding of aluminum alloy, the instability is

Table 2 Experimental group

Experimental group	A1	A2	A3	A4	A5	A6
Laser power (W)	2200	2200	2200	2600	2600	2600
Magnetic field intensity (mT)	0	114	188	0	114	188

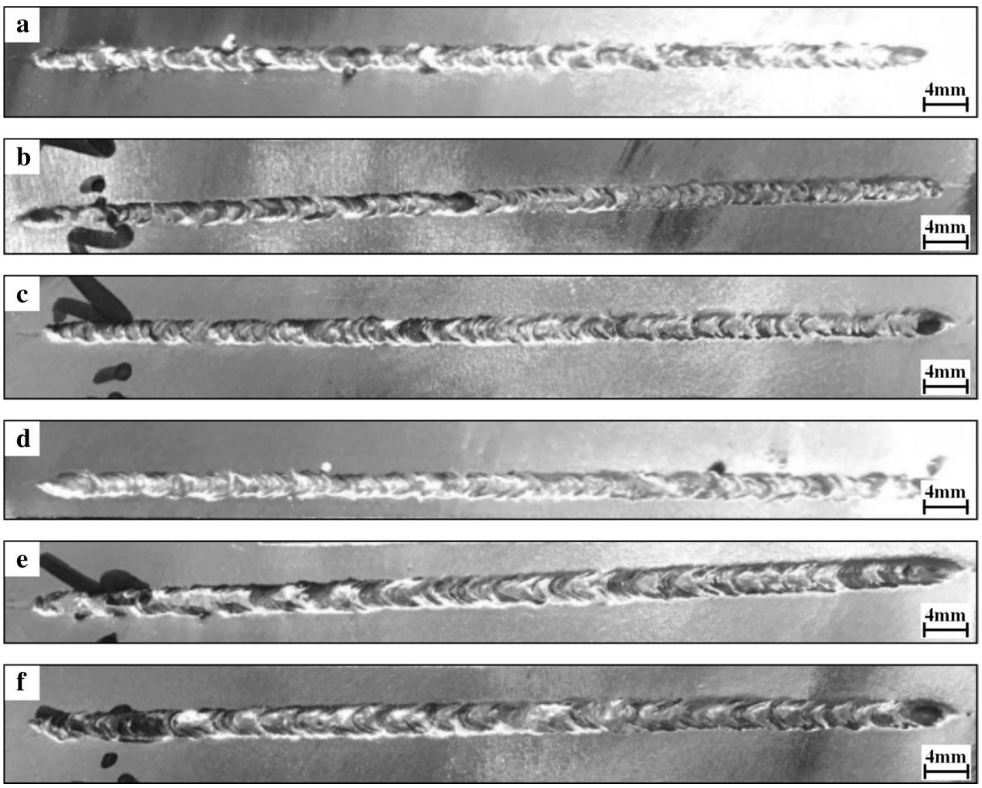

Fig. 4 2024 aluminum alloy weld surface morphology: **a–f** group A1–A6

ineluctable due to the low viscosity of the liquid aluminum which can promote highly dynamical processes near the surfaces. However, the spattering is reduced and the surface morphology is improved after the application of magnetic field, but these effects are not obvious as shown in Fig. 4b, c, e, f. Because of the interaction of Marangoni convection and externally applied magnetic field, the produced Lorentz force which is directed against the fluid flow is opposite to the direction of Marangoni convection. The welding spattering has been reduced, but the interaction is small due to the low laser power.

The weld cross section of non-magnetic field when the laser power is 2200 W is shown in Fig. 5a; it is obvious that the weld seam is in the state of incomplete penetration.

The magnetic field has no obvious influence on the morphology of cross section as shown in Fig. 5b, c. The reason is that small laser power leads to a low heat input, and the laser interacts with aluminum and forms a keyhole. Since the temperature gradient from the keyhole to the edge of the molten pool and the surface tension gradient are small, the Marangoni convection intensity near surface by which weld cross section morphology is mainly concerned is weak. However, even in the weak intensity, the morphology is still in the wineglass-shape. During the welding process with the magnetic field, the Lorentz force formed through the interaction of Marangoni convection and externally applied magnetic field is week due to the weak Marangoni convection intensity. The dissipating effect is not obvious, and the morphology is still in the wineglass-shape.

Further, the weld cross section under the effect of magnetic field when the laser power is 2600 W is shown in Fig. 5a; it is obvious that the weld seam is in the state of complete penetration. With the application of magnetic field in the welding process and increase of the magnetic field strength, that is from 0 to 114 and 188 mT, the cross section morphology is gradually changed from the wineglass-shape to the cone shape. In addition, the weld width near the surface is also significantly reduced as shown in Fig. 5e, f. High heat input leads to a steep temperature gradient and tension gradient on the surface of weld pool, and the Marangoni convection intensity is much stronger

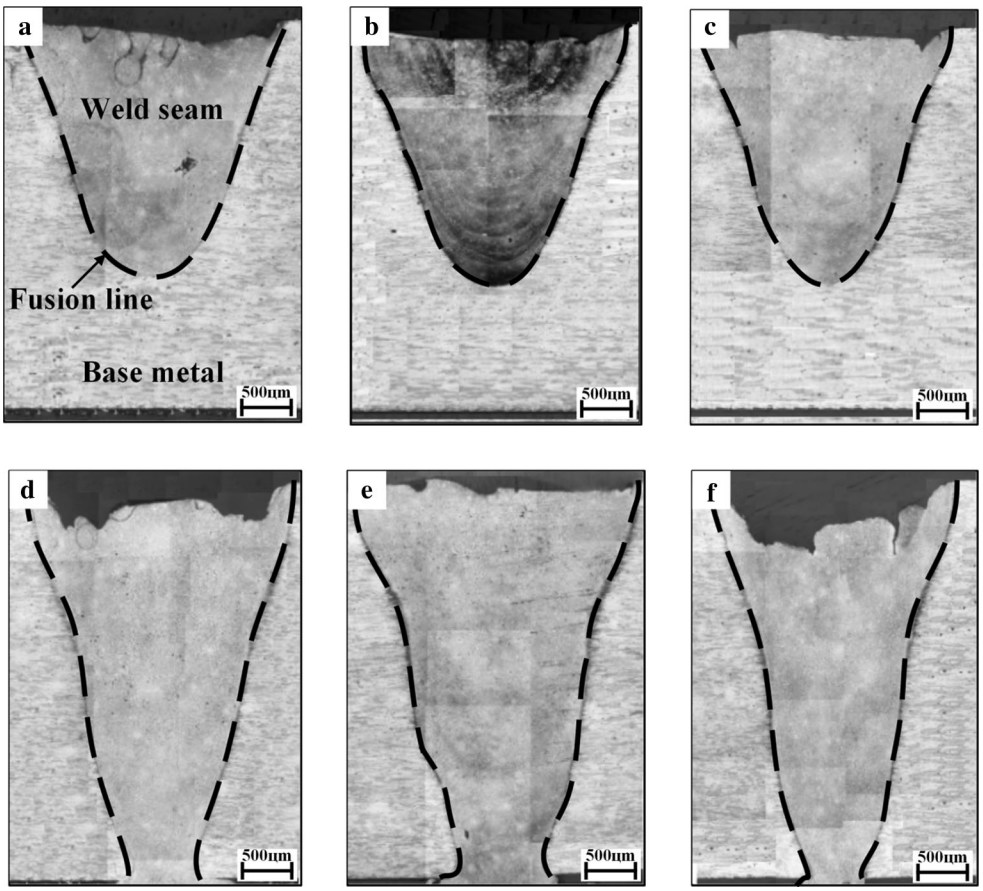

Fig. 5 2024 aluminum alloy weld cross section morphology: **a–f** group A1–A6

than in 2200 W. Although the strength of the magnetic field is the same, due to the increase of the Marangoni convection intensity, the Lorentz force which can astrict the Marangoni convection becomes much stronger and the dissipating effect is obvious too. It is shown with the change from the wineglass-shape to the cone shape. In addition, the weld width of surface is closely related to the strength of Marangoni convection too, when the laser power is 2600 W, Marangoni convection is significantly astricted by applied magnetic field. Thereafter, with the increase of magnetic field intensity, the weld width of surface also has an obvious reduction.

To obtain a more profound understanding about the influence of the magnetic field on the macrostructure of the weld seam, the width-to-depth change ratio R was measured through

$$\varphi = \frac{B}{H} \tag{3}$$

$$R = \frac{|\varphi_1 - \varphi_0|}{\varphi_0} \tag{4}$$

with B, H and φ, respectively, being the weld width, weld penetration depth and width-to-depth ratio. And the φ_1 and φ_2, respectively, are the width-to-depth ratios on the effect of magnetic field and non-magnetic field. As shown in Fig. 6b, R shifts from 0 to 2.0 to 5.9% with the magnetic field intensity varying from 0 to 114 to 188 mT when the laser power is 2200 W (groups 1, 2 and 3). Particularly, when the laser power is increased, the change rate of R is obviously increased, that is from 0 to 4.8 to 12.9% with the magnetic field intensity varying from 0 to 114 to 188 mT. The width-to-depth change ratio shows that the weld formation is affected by the additional external magnetic fields. Moreover, this effect is obviously enhanced with the augmentation of laser power.

In addition, the measurement of the width at different depths was taken. The schematic diagram and the results of measuring the weld width are shown in Fig. 7. As shown in Fig. 7a, the weld width has no significant reduction with the increase of the magnetic field strength. Since the Marangoni convection intensity near the surface is week and the dissipating effect is not obvious, the effect of other factors such as protective gas interference on the fluid flow in the molten pool is relatively more obvious. Hence, the weld width reduces inconspicuously.

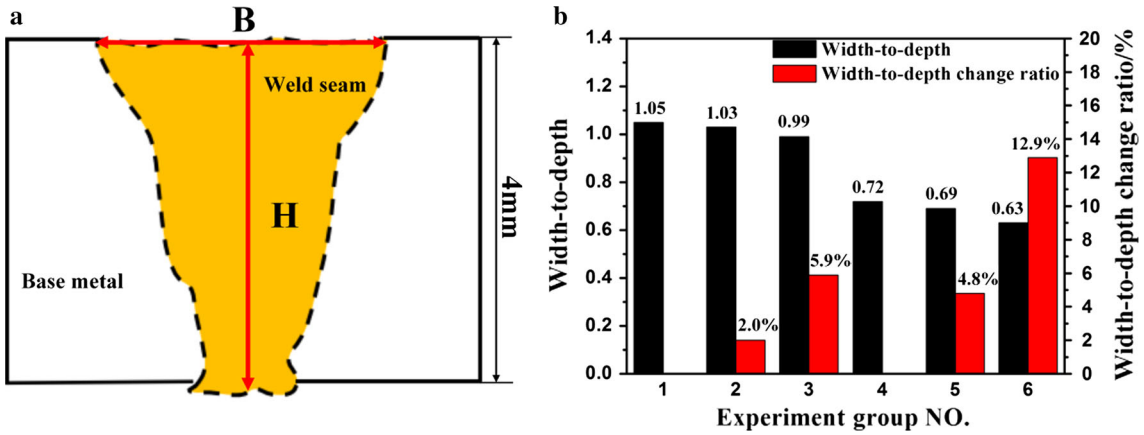

Fig. 6 The measuring position and the width-to-depth ratio and change ratio under different process conditions

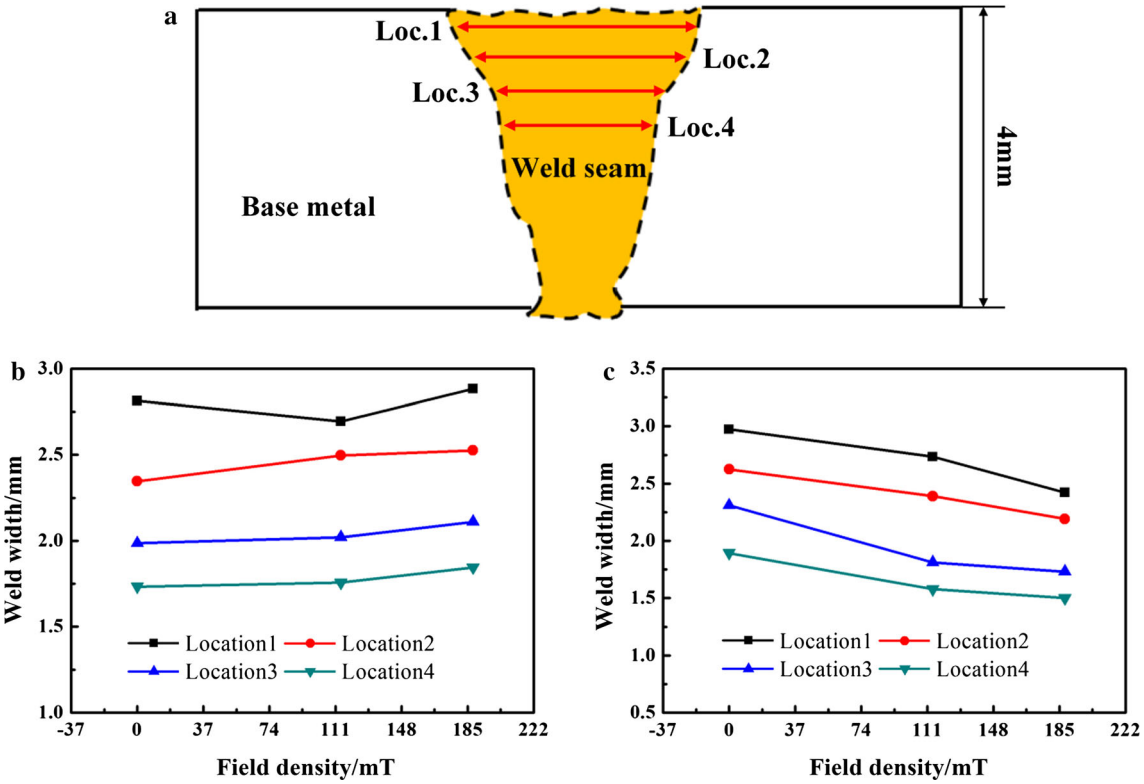

Fig. 7 The weld width measuring position and the weld width of each location with the magnetic field: **a** group A1–A3; **b** group A4–A6

The weld width changes are different when the laser power is 2600 W as shown in Fig. 7b. The weld width obviously decreased with the increase of the magnetic field strength, especially near the surface. Additionally, with the increase of laser power, the convection intensity of molten pool also increased, which leads to the interaction of magnetic field and convection to a high level, so the suppression effect of magnetic field is more obvious. In particular, the weld width of the location 1 reduced most obviously, where the convection intensity of Marangoni and the suppression effect of the magnetic field are the largest.

4 Discussion

It is well known that the suppression on convection has a significant effect on the crystallization process [30]. In order to find an exact and convective explanation on macro-performance (weld formation, cross section and

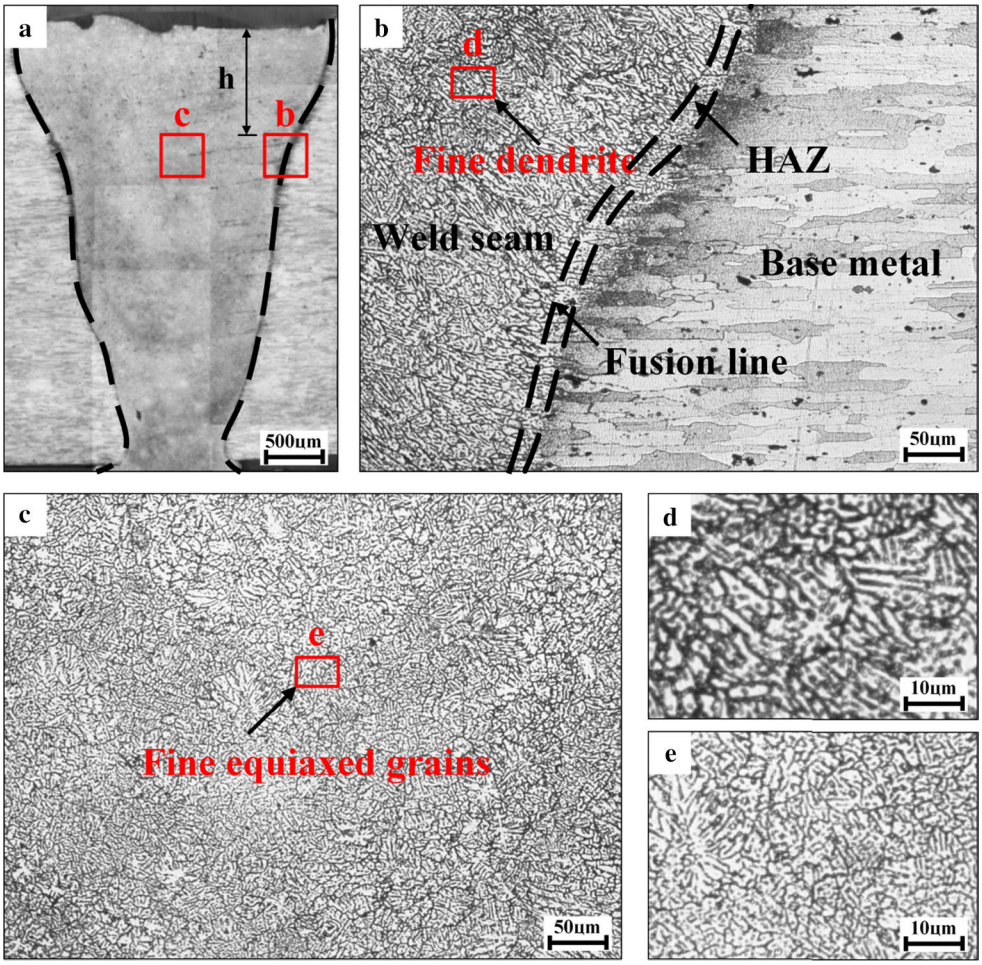

Fig. 8 Microstructure of the center of weld pool and the vicinity of the fusion line of group A4

width-to-depth ratio) after the application of magnetic field, the micro-analysis is studied in this part. Considering that Marangoni convection occurred near the surface of the weld pool, the sampling location is chosen in the upper portion of weld seam. The experiments are measured by an optical microscope.

Figures 8a and 9a represent four micro-regions distributed along the right fusion line and in the weld center with same distances ($h = 608$ μm) from the weld surface. As shown in Figs. 8b and 9b, overall, it was observed that the size of the cellular dendrites on the weld edge of group 6 was coarsened compared to group 4. For characterization of the variations, a further observation was captured. The exact sampling locations were shown in region *d*. The detailed microstructures are shown in Figs. 8d and 9d.

The change of grain size shows that the crystallization of the molten pool is hindered by the effect of magnetic field. There are several mechanisms involved in the formation of new substrates to enhance the nucleation of new grains in the weld pool, that is heterogeneous nucleation, grain detachment, dendrite fragmentation and surface nucleation [30]. The grain detachment and dendrite fragmentation are closely related to the Marangoni convection. Hence, when the magnetic field is applied, the cellular dendrites were coarsened duo to the inhibition of these two mechanisms by the interaction of Marangoni convection and externally applied magnetic field as shown in Fig. 9b, d. However, under the direct effect of laser beam in the center of weld pool, the suppression of magnetic field is not obvious; hence, the difference of microstructure in the center of weld pool is not obvious as shown in Figs. 8e and 9e.

Additionally, the distribution of components is affected by the influence of the magnetic field on the convection too [27]; it is analyzed by the X-ray line scan of electron probe microstructural analysis from the center of the weld to the base metal as shown in Figs. 10 and 11.

Figure 10b shows the content of main alloy component Mg of the experimental group A4, and it reveals that the Mg component average content has no obvious change trend from the center of the weld to the base metal. On the contrary, an increasing trend of the Mg component average content was measured of group A6 from the center of the

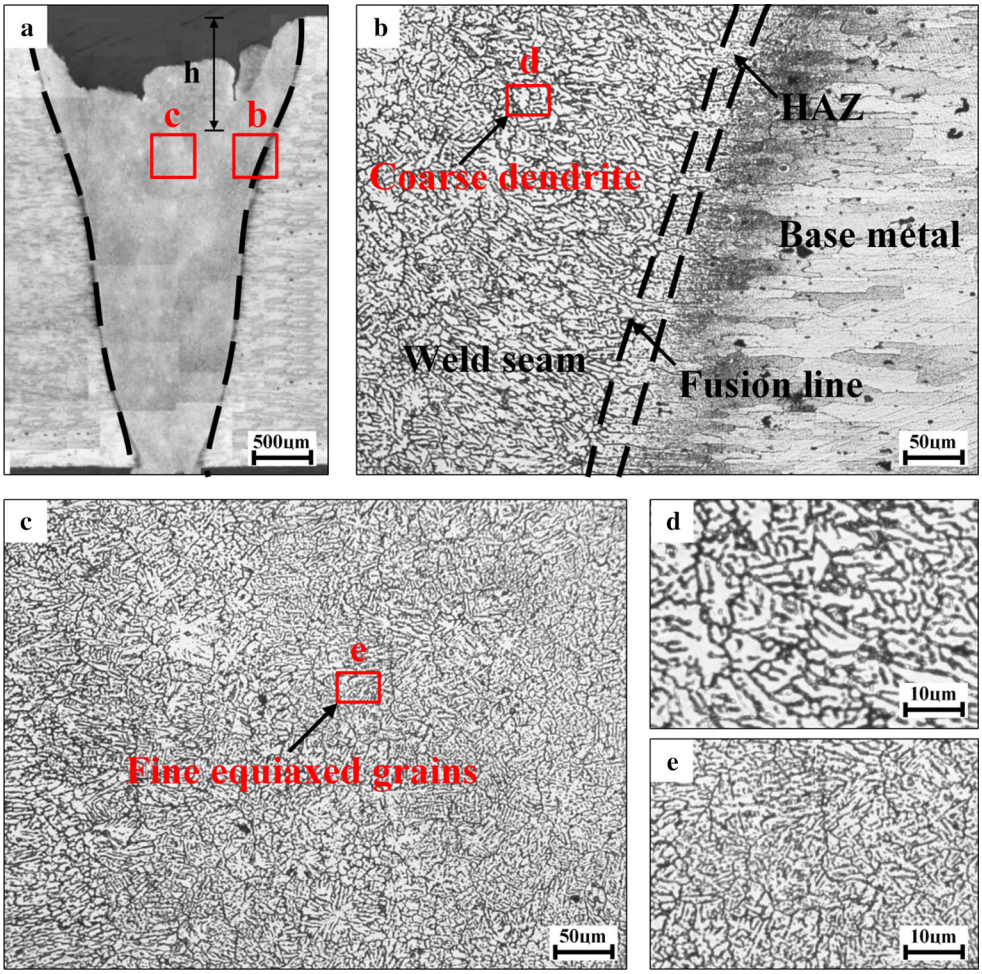

Fig. 9 Microstructure of the center of weld pool and the vicinity of the fusion line of group A6

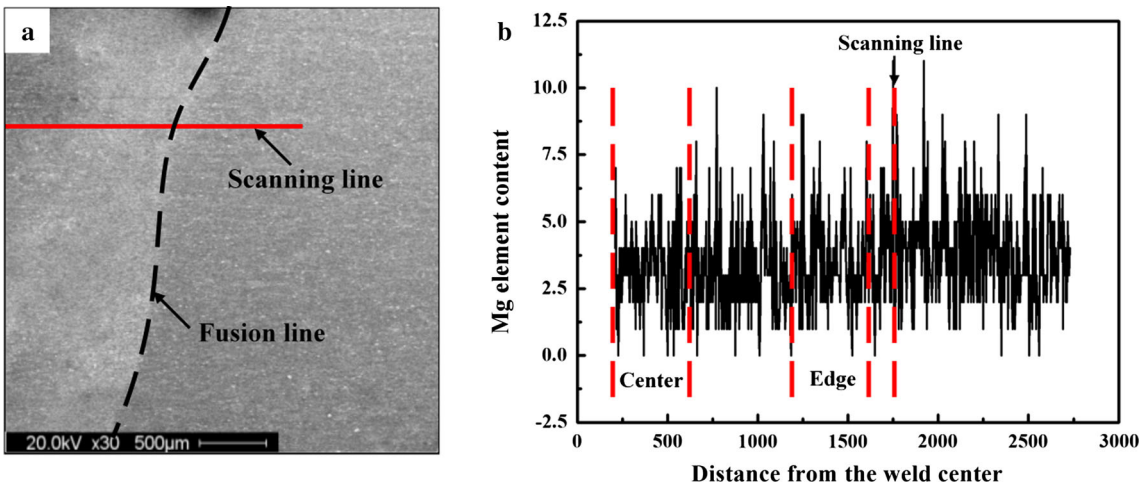

Fig. 10 Distribution of components from the weld center to the base metal of group A4

weld to the base metal as shown in Fig. 11b. With the action of the external magnetic field, the convection velocity decreases. In the case of the same total amount of the component, the component is enriched near the fusion line more easily. However, since the laser power is small, the suppression of the magnetic field on the convection is not strong, resulting in the change trend of the Mg component which is not very obvious.

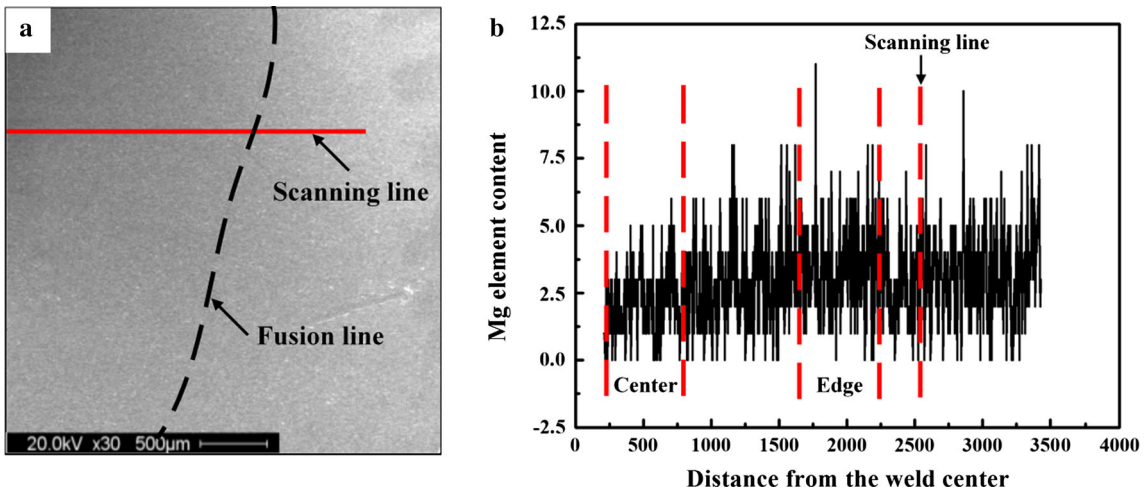

Fig. 11 Distribution of components from the weld center to the base metal of group A6

The suppression effect of the magnetic field is indirectly confirmed by the comparison on the grain size and the component concentration distributions between non-magnetic field and magnetic field. It is undisputed that the steady magnetic field plays an important role in the influence on the convection. As mentioned earlier, the weld surface, cross sections and form factor associated with convections are availably improved.

5 Conclusions

The influence of additional steady transverse magnetic field on weld formation, weld microstructure and Mg component distribution of aluminum alloy 2024 laser-welded joints was investigated using experimental and theoretical methods. The conclusions could be drawn as follows:

1. The additional steady transverse magnetic field has obvious inhibitory influence, and the solidification microstructure is affected to be more regular. In the influence of additional magnetic field, the morphology in the cross section of weld joint is gradually changed from the wineglass-shape to the cone shape after cooling.
2. The suppression of the Marangoni convection by the additional magnetic field not only affects the morphology of the welded joint, but also affects the weld width. When the laser power is larger, with the increase of the magnetic field intensity, the weld width of the near surface is reduced significantly.
3. Particularly, the weld formation is affected by the additional external magnetic fields. Moreover, this effect is obviously enhanced with the augmentation of laser power. The width-to-depth change ratio shifts from 0 to 2.0 to 5.9% with the magnetic field intensity varying from 0 to 114 to 188 mT when the laser power is 2200 W. With the increasing of laser power, the change rate of R is obviously increased, that is from 0 to 4.8 to 12.9% with the magnetic field intensity varying from 0 to 114 to 188 mT.
4. In addition, the magnetic field can affect the crystallization process near the fusion line in the top part of the weld pool. The nucleation of grains in the weld pool has been relatively limited, and it results in the coarsening of the gain. At the same time, the composition segregation is founded near the fusion line more due to the inhibiting effect of magnetic field.
5. The inhibiting effect of the applied steady magnetic field on the convection of the molten pool in the laser welding process of aluminum alloy is also obviously related to the laser power. In a low level of laser power, the Marangoni convection strength near the weld pool surface is week, the interference of other factors such as the influence of protective gas is relatively non-ignorable. Therefore, when the laser power of 2200 W, the weld morphology changes were not observed obviously.

Acknowledgements The authors gratefully acknowledge the financial support of the project from the National Commercial Aircraft Manufacturing Engineering Technology Research Center Innovation Fund of China (SAMC14-JS-15-052), National Science Foundation of China (No. U1637103) and a Project Funded by the Priority Academic Program Development of Jiangsu Higher Education Institutions (PAPD).

References

1. W.S. Miller, L. Zhuang, J. Bottema et al., Recent development in aluminium alloys for the automotive industry. Mater. Sci. Eng., A **280**(1), 37–49 (2000)

2. M. Suzuki, A Japanese perspective on the use of aluminium alloys in the automotive sector. Mater. Sci. Forum **519**, 11–14 (2006)
3. N. Nadammal, S.V. Kailas, S. Suwas, A bottom-up approach for optimization of friction stir processing parameters; a study on aluminium 2024-T3 alloy. Mater. Des. **65**, 127–138 (2015)
4. S. Lathabai, B.L. Jarvis, K.J. Barton, Keyhole gas tungsten arc welding of commercially pure zirconium. Sci. Technol. Weld. Join. **13**(6), 573–581 (2008)
5. S. Lathabai, B.L. Jarvis, K.J. Barton, Comparison of keyhole and conventional gas tungsten arc welds in commercially pure titanium. Mater. Sci. Eng., A **299**(1–2), 81–93 (2001)
6. M. Sheikhi, F.M. Ghaini, H. Assadi, Prediction of solidification cracking in pulsed laser welding of 2024 aluminum alloy. Acta Mater. **82**, 491–502 (2015)
7. M. Pastor, H. Zhao, R.P. Martukanitz et al., Porosity, underfill and magnesium loss during continuous wave Nd:YAG laser welding of thin plates of aluminum alloys 5182 and 5754. Weld. J. **78**(6), 207s–216s (1999)
8. B. Chang, C. Allen, J. Blackburn et al., Thermal and fluid flow characteristics and their relationships with porosity in laser welding of AA5083. Phys. Proced. **41**, 478–487 (2013)
9. M. Windmann, A. Röttger, H. Kügler et al., Removal of oxides and brittle coating constituents at the surface of coated hot-forming 22MnB5 steel for a laser welding process with aluminum alloys. Surf. Coat. Technol. **285**, 153–160 (2016)
10. F. Caiazzo, V. Alfieri, F. Cardaropoli et al., Butt autogenous laser welding of AA 2024 aluminium alloy thin sheets with a Yb:YAG disk laser. Int. J. Adv. Manuf. Technol. **67**(9–12), 2157–2169 (2013)
11. J. Enz, V. Khomenko, S. Riekehr et al., Single-sided laser beam welding of a dissimilar AA2024–AA7050 T-joint. Mater. Des. **76**, 110–116 (2015)
12. A. Matsunawa, Problems and solutions in deep penetration laser welding. Sci. Technol. Weld. Join. **6**(6), 351–354 (2001)
13. D.I.H.D. Radaj, *Welding residual stress and distortion: heat effects of welding* (Springer, Berlin Heidelberg, 1992), pp. 129–246
14. H.K. Moffatt, Electromagnetic stirring. Phys. Fluids A Fluids Dyn **3**(5), 1336–1343 (1991)
15. V.V. Avilov, A. Gumenyuk, M. Lammers et al., PA position full penetration high power laser beam welding of up to 30 mm thick AlMg3 plates using electromagnetic weld pool support. Sci. Technol. Weld. Join. **17**(2), 128–133 (2013)
16. P. Rudolph, Travelling magnetic fields applied to bulk crystal growth from the melt: the step from basic research to industrial scale. J. Cryst. Growth **310**(7–9), 1298–1306 (2008)
17. M. Bachmann, V. Avilov, A. Gumenyuk et al., Numerical simulation of full-penetration laser beam welding of thick aluminium plates with inductive support. J. Phys. D Appl. Phys. **45**(3), 35201–35213 (2011)
18. V. Avilov, A. Schneider, M. Lammers et al., Electromagnetic control of the weld pool dynamics in partial penetration laser beam welding of aluminium alloys. J. Iron. Steel Res. Int. **S1**, 233–236 (2012)
19. M. Bachmann, V. Avilov, A. Gumenyuk et al., About the influence of a steady magnetic field on weld pool dynamics in partial penetration high power laser beam welding of thick aluminium parts. Int. J. Heat Mass Transf. **60**(60), 309–321 (2013)
20. N. Barman, P. Kumar, P. Dutta, Studies on transport phenomena during solidification of an aluminum alloy in the presence of linear electromagnetic stirring. J. Mater. Process. Technol. **209**(18), 5912–5923 (2009). doi:10.1016/j.jmatprotec.2009.07.008
21. M. Sommer, J.P. Weberpals, S. Müller, et al. Advantages of laser beam oscillation for remote welding of aluminum closely above the deep-penetration welding threshold. J. Laser Appl. **29** (2017)
22. O. Velde, A. Techel, R. Grundmann, Suppression of the development of pores during laser-induced surface dispersion of TiC into aluminium, by means of a static magnetic field. Surf. Coat. Technol. **150**(2–3), 170–176 (2002)
23. M. Gatzen, Z. Tang, F. Vollertsen et al., X-ray investigation of melt flow behavior under magnetic stirring regime in laser beam welding of aluminum. J. Laser Appl. **23**(3), 032002 (2011)
24. A. Schneider, V. Avilov, A. Gumenyuk et al., Laser beam welding of aluminum alloys under the influence of an electromagnetic field. Phys. Proced. **41**(30), 4–11 (2013)
25. E.H. Amara, A. Bendib, Modelling of vapour flow in deep penetration laser welding. J. Phys. D Appl. Phys. **35**(3), 272–280 (2002)
26. E.H. Amara, R. Fabbro, Modelling of gas jet effect on the melt pool movements during deep penetration laser welding. J. Phys. D Appl. Phys. **41**(41), 455–457 (2008)
27. M. Gatzen, Z. Tang, F. Vollertsen, Effect of electromagnetic stirring on the element distribution in laser beam welding of aluminium with filler wire. Phys. Proced. **12**(1), 56–65 (2011)
28. S. Kou, Y.H. Wang, Three-dimensional convection in laser melted pools. Metall. Trans. A **17**(12), 2265–2270 (1986)
29. M. Gatzen, Z. Tang, CFD-based model for melt flow in laser beam welding of aluminium with coaxial magnetic field. Phys. Proced. **5**, 317–326 (2010)
30. M.G. Mousavi, M.J.M. Hermans, I.M. Richardson et al., Grain refinement due to grain detachment in electromagnetically stirred AA7020 welds. Sci. Technol. Weld. Join. **8**(4), 309–312 (2003)